Publishing House
AKAPIT

COMPUTER METHODS IN MATERIALS SCIENCE

Informatyka w Technologii Materiałów

Vol. 10, 2010, No. 3

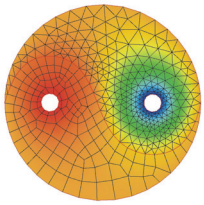

NUMERICAL SIMULATION OF VISCOELASTIC EFFECTS IN BLADE-OVER-ROLL COATING FORMING FLOWS

EVAN MITSOULIS

School of Mining Engineering and Metallurgy,
National Technical University of Athens,
Zografou 157 80, Athens, GREECE
e-mail: mitsouli@metal.ntua.gr

Abstract

Computer simulations of the blade-over-roll coating process so far have been based mostly on Newtonian or generalized Newtonian models, which do not take into account the viscoelasticity of coating materials. Strong viscoelastic effects can influence both the flow characteristics in a blade nip and the coating film thickness. Because of limitations of the constitutive equation which describes coating materials, comparisons of simulation results with experiments had limited success. We have simulated the coating process with a fixed blade using the finite element method (FEM). Newtonian data are well reproduced by using a full two-dimensional model with realistic boundary conditions. For the case of viscoelastic fluids, i.e., polymer solutions with either a constant viscosity (Boger fluids) or a shear-thinning one, we used an integral constitutive equation of the K-BKZ type. Key characteristics of the K-BKZ model are that it accounts for a spectrum of multiple relaxation parameters and a fading memory. Numerical results accurately predict the coating film thicknesses from experiments reported in the literature. For a given geometry and speed, the film thickness decreases with increasing viscoelastic behavior. This is particularly evident when comparing the film thicknesses of the Newtonian and Boger fluids. Results show that the K-BKZ viscoelastic model is adequate to capture memory phenomena associated with the strain history of homogeneous polymeric coating materials, and can have application to simulating paper coating dispersions.

Key words: coating flows; blade-and-roll coating; K-BKZ constitutive equation; viscoelasticity; rheology

1. INTRODUCTION

Blade-coating flows are of particular interest in the application of very small volumes of liquids and dispersions coated on extremely thin layers over moving substrates. The blade is used to control the coating thickness and produce a uniformly smooth surface. However, due to the non-Newtonian nature of the applied material, the coating thickness is not equal to the separation gap between the blade tip and the substrate. The movement of the material under the blade is being characterized by a drag, which retards the flow, and a pressure gradient which pumps material in the direction of the substrate movement. Therefore, the flow is a combination of Couette (velocity-driven) and Poiseuille (pressure-driven) flows. The actual coating thickness depends on blade design geometry, operational conditions, the rheology of the applied material, and, for the case of paper coating, the absorptivity and compressibility of the substrate. Here we are focusing on a metering blade nip having a fixed geometry, fluid continua with viscoelastic properties, and a non-absorptive, incompressible substrate.

Analyses of the blade-coating process so far have been based mostly on Newtonian or generalized non-Newtonian models (Kistler & Scriven, 1984; Mitsoulis & Athanasopoulos, 2010), which do

 ISSN 1641-8581

not take into account the non-Newtonian nature and viscoelasticity of many coating liquids (Sullivan et al., 1987). The problem is compounded by the presence of free surfaces, both upstream of the substrate and downstream of where the actual coating takes place (figure 1). Typically, for a Newtonian fluid, the coating thickness is one half the thickness of the gap between the blade tip and the substrate. Although analysis of the flow using perturbation theory to solve the Navier-Stokes equations based on the lubrication theory gives solutions which agree with experiments of Newtonian fluids, this is not true for the case of viscoelastic materials (Hsu et al., 1985). High elastic stresses, comparable to purely shear stresses, increase the separating force which tends to push the bounding surfaces of the flow apart. The separating force also increases proportionally to flow velocity. When the material is being described as a purely viscous fluid, only an order-of-magnitude agreement has been obtained between experiment and analysis using perturbation theory (Hsu, 1986). Accurate description of the rheology of coating materials is therefore crucial is assessing their behavior in blade coating.

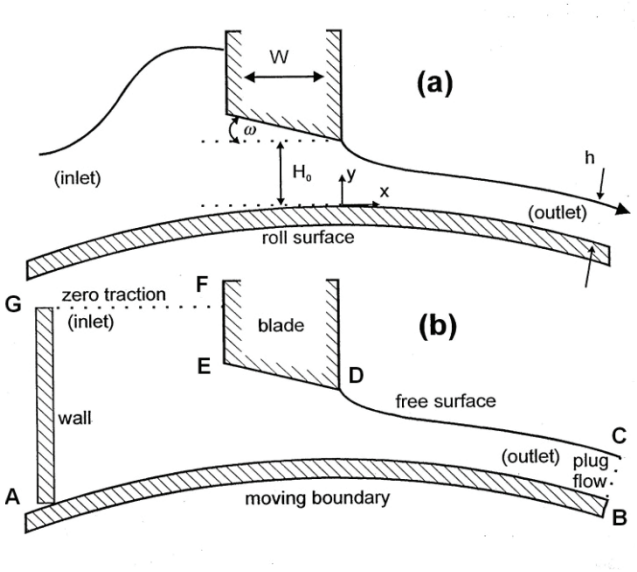

Fig. 1. *(a) Schematic diagram of the fixed blade-over-roll coater domain with relevant notation; (b) the simulation flow domain with the addition of a reservoir wall upstream and relevant boundary conditions.*

Rheological effects play a significant role in determining the coating film thickness and its uniformity. Elasticity increases the normal stresses under the blade and affects blade loading, while shear-thinning influences the flow and the pressure distributions. Greener and Middleman (1974) demonstrated with a theoretical analysis that viscoelastic effects significantly reduce blade loading. They found that quantitatively the influence on coating thickness depends on the selected constitutive equation, which defines the rheology of non-Newtonian fluids, since elastic Newtonian fluids (i.e., a "Boger" fluid, such as a polyacrylamide solution in corn syrup) exhibited an increase in blade coating relative to a Newtonian fluid. Therefore, the choice of the constitutive equation used to describe the coating material is critical to accurately investigate the influence of viscoelasticity in coating flows.

Detailed computer simulation and experimental studies by Sullivan et al. (1987), and Sullivan and Middleman (1986) investigated the influence of non-Newtonian rheology on the flow patterns and coating thickness. Shear-thinning and elasticity compete with respect to their influence on coating thickness. Purely shear-thinning inelastic materials, such as a dilute solution of low-molecular weight carboxymethyl-cellulose (CMC), increase the film thickness relative to a Newtonian fluid. Elasticity, induced by adding high-molecular weight polyacrylamide (PAA) to the CMC solution, reduces the film thickness. Reduction in film thickness was also observed with a Boger fluid; a constant-viscosity fluid with elasticity described in detail below. While for purely shear-thinning fluid the film thickness was dependent on blade geometry (i.e, blade tip angle and thickness), there was little dependence on geometry in the case of a Boger fluid. In addition to their influence on coating thickness, elastic effects were also found to shrink the operational window of blade coating, primarily through the appearance of the ribbing effect due to the presence of normal forces (Strenger et al., 1992). Numerical simulations by Olsson (1994) and Olsson and Isaaksson (1995) demonstrated that the total force acting on a stationary blade is lower for viscoelastic than Newtonian fluids due to the rapidly reduced normal force with the distance downstream. There is also a tendency of viscoelastic fluids to "clog" the flow at the entry to the blade nip channel, causing formation of counter-rotating vortices at the boundary layer on the under face of the blade. The low normal forces observed by these authors, however, contradict previous results by Hsu (1986), who found the normal force to significantly increase with elasticity. Differences in the assumed constitutive equation describing the rheology of the coating material can possibly explain the results of the two studies.

A major issue in reconciling simulation results with experiments is the accurate representation of viscoelasticity through utilization of appropriate

constitutive equations (Mitsoulis, 1990). Sullivan et al. (1987) utilized the three-parameter Carreau model, while Olsson (1994) used the Oldroyd-B and Giesekus models. However, numerical results only partly agreed with experiments from these and other authors. In the mid-1980's progress was achieved in the viscoelastic simulation of polymeric materials by using constitutive equations of the K-BKZ type (Papanastasiou et al., 1983; Luo & Tanner, 1986). This type of constitutive equation has been named after Bernstein et al. (1963), who first introduced it for modeling polymer solutions and melts with a spectrum of relaxation times. The K-BKZ model has been successfully used to describe the melt rheology of low- and high-density polyethylenes (LDPE, HDPE), polystyrene (PS), polypropylene (PP), and the solution rheology of polyacrylamide (PAA) and polyisobutylene (PIB) (Kajiwara et al., 1995). Numerical techniques based on FEM using the K-BKZ model have been developed to handle particle tracking in the general case of flows with open and closed streamlines (Dupont & Crochet, 1988; Luo & Mitsoulis, 1990a). Test cases for commercial polyethylene melts in relatively simple geometries, such as abrupt contractions (Dupont & Crochet, 1988; Luo & Mitsoulis, 1990a; 1990b) and extrusion through dies (Luo & Tanner, 1988; Luo & Mitsoulis, 1989) have shown the adequacy of the integral model to capture memory phenomena and strong viscoelastic behavior, not seen with the simple models of the Maxwell or Oldroyd-B type.

This integral model has been used continuously in the 1990's and 2000's in numerical flow simulations for a number of flow problems more or less successfully (see, e.g. Park & Mitsoulis, 1992; Barakos & Mitsoulis, 1995; Sun et al., 1996a; Mitsoulis & Hatzikiriakos, 2003; Mitsoulis, 2010; Ansari et al., 2010). A review (Keunings, 2003) on the subject gives a list of problems solved with this model through numerical simulation, including many flows from polymer-processing operations. However, for viscoelastic fluids, coating flows have not been analyzed with the K-BKZ model so far.

In the present work we used the K-BKZ integral constitutive equation to study the flow behavior of the viscoelastic polymer solutions used in the experimental investigation by Sullivan et al. (1987), and Sullivan and Middleman (1986). The emphasis is on the viscoelastic nature of polymeric solutions and how it affects the blade-coating process. In most operations of practical interest, these effects are dramatic and cannot be captured by Newtonian fluid dynamics or simplified models, such as the power-law model for shear-thinning behavior.

2. MATHEMATICAL MODELLING OF COATING FLOWS

2.1. Conservation and constitutive equations

The coating flow between a moving substrate and a stationary doctor blade for incompressible fluids (such as polymer solutions) under isothermal and steady-state conditions is governed by the usual conservation equations of mass and momentum (Sullivan et al., 1987), i.e.,

$$\nabla \cdot \boldsymbol{v} = 0 \tag{1}$$

$$\rho \boldsymbol{v} \cdot \nabla \boldsymbol{v} = -\nabla p + \nabla \cdot \boldsymbol{\tau} \tag{2}$$

where v is the velocity vector, p is the scalar pressure, τ is the extra stress tensor, and ρ is the density.

The constitutive equation that relates the stresses τ to the deformation history is the K-BKZ model. This phenomenological model draws from the theory of rubber elasticity and it accounts for nonlinear effects arising from the interactions of polymer chains. Most importantly, it includes a spectrum of material relaxation times, in contrast to purely viscous models of the power-law or the Carreau type, which are only sufficient for representing the steady shear viscosity of the material (Mitsoulis & Athanasopoulos, 2010). In contrast to implicit differential models, the K-BKZ model involves an integral equation which reduces to the linear Maxwell and Oldroyd-B models by choosing a single relaxation time and a constant viscosity. It gives similar predictions to the Phan-Thien/Tanner (PTT) and Giesekus models, provided that the latter are being written for multiple modes having a spectrum of relaxation times.

The form of the K-BKZ model we used is based on the equation proposed by Papanastasiou et al. (1983), and further modified by Luo and Tanner (1988):

$$\tau = \frac{1}{1-\theta}\int_{-\infty}^{t}\sum_{k=1}^{N}\frac{a_k}{\lambda_k}\exp\left(-\frac{t-t'}{\lambda_k}\right)$$

$$\frac{\alpha}{(\alpha-3)+\beta_k I_{C^{-1}}+(1-\beta_k)I_C}\left(C_t^{-1}(t')+\theta C_t(t')\right)dt' \tag{3}$$

In the above, N is the number of relaxation modes, λ_k and a_k are the relaxation times and relaxation modulus coefficients at a reference temperature, α, β and θ are material constants, and I_C and I_C^{-1} are the first invariants of the Cauchy-Green tensor C_t and its inverse C_t^{-1}, the Finger strain tensor. The material constant θ is given by

$$\frac{N_2}{N_1} = \frac{\theta}{1-\theta}, \tag{4}$$

where N_1 and N_2 are the first and second normal stress differences, respectively. It is noted that θ is not zero for polymer solutions, such as the solutions of PAA and the Boger fluid discussed here, which possess a non-zero second normal stress difference. Typical values for θ are in the range between –0.1 and –0.2 in accordance with experimental findings (Dealy & Wissbrun, 1990). For the present work, a value of $\theta = -1/9$ (N_2/N_1=–0.1) has been used.

2.2. Boundary conditions

The flow boundary conditions (see figure 1b) have been fully described in our previous paper (Mitsoulis & Athanasopoulos, 2010) and are not repeated here. Note that at point A there is a *singularity*, because mathematically the same node has a zero velocity if it belongs to the reservoir wall GA and a finite V_R velocity if it belongs to the moving roll surface AB. Practically, there is a very small gap between the reservoir wall and the roll to allow for the roll motion. Numerically, we set very small elements around the corner node and set the corner node (point A) as a wall node (zero velocity) and the next node on the roll we set equal to the roll speed. This has been found to be the best way to handle the singularity (Mitsoulis et al., 1988; Loest et al., 1994), which otherwise may affect grossly the results (loss of mass flow rate).

In general, there are three *singularities* in this flow field: (a) at blade corner of point E, where the velocity is zero but the derivatives are discontinuous (zero-order singularity, flow around a corner wall); (b) at blade corner of point D, where the velocity is discontinuous changing *smoothly* from zero to a non-zero value due to the free surface (first-order singularity, flow at a solid/gas interface); and (c) at point A, where the wall meets a solid moving boundary and the velocity is discontinuous changing *abruptly* from zero to a distinct non-zero value (second-order singularity, flow from a non-moving to a moving boundary). This last one is the most severe and causes the most trouble numerically if not adequately handled.

For the simulations, all lengths have been made dimensionless by the minimum gap H_0, all velocities by the roll speed V_R, and all stresses and pressures by $\eta_0 V_R/H_0$.

3. RHEOLOGICAL CHARACTERIZATION

The materials used to validate the simulation results with experiments in blade-coating flow were dilute polymer solutions, as described by Sullivan et al. (1987). The solutions were prepared by first dissolving CMC (1.25% wt) in distilled water. Because of their low polymer concentration, the solutions are considered inelastic, shear-thinning fluids (figure 2). They become viscoelastic by adding small amounts of polyacrylamide (PAA). For the CMC solutions containing PAA (i.e., CMC fluids 1 through 3), the flow behavior is being determined by the interaction between shear-rate dependent viscosity, fluid inertia, and fluid elasticity. In addition to the CMC fluids 1 through 3, we also considered an aqueous solution (96.3% wt) of corn syrup with 500 ppm PAA. This is a constant-viscosity (Newtonian) but highly elastic fluid, the so-called Boger fluid (Boger, 1977/1978; Mitsoulis, 2010). This model fluid is typically being produced by dissolving a high molecular weight polymer (i.e., PAA) at low concentration in a highly viscous Newtonian fluid (i.e., corn syrup), thereby masking the shear-rate dependent viscosity contribution of the polymer (Boger, 1977/1978). Although the solution in fact displays shear-thinning, the reduction in viscosity is very small compared to the zero-shear viscosity value, and, for all practical purposes, the viscosity remains constant. A Boger fluid allows assessing the influence of elasticity without the "interference" of non-Newtonian (shear-thinning) viscous effects.

Detailed rheological data are given for the shear viscosity and the first normal stress difference, and are shown in figure 2. First, we note that the shear viscosity is not affected very much, and for comparison purposes it can be also represented by the Carreau model (Mitsoulis & Athanasopoulos, 2010). Using the viscoelastic model of equation 3, a nonlinear regression analysis was performed according to the method described by Kajiwara et al. (1995) for the determination of the relaxation spectrum constants and the other material parameters. Solid lines in figure 2 represent the best-fit curves to the data.

Due to lack of elongational viscosity data for the polymer solutions, we have used a constant β-value for the elongational parameter of the model. In the simulations we have used a second normal stress difference term involving a constant θ-value. The values of the parameters are given in tables 1-4. Four characteristic relaxation times are used for the shear-thinning viscoelastic polymer solutions, while two relaxation times are adequate to describe the behavior of the constant-viscosity Boger fluid (Mitsoulis, 2010). As pointed out by Kajiwara et al. (1995), it is possible with these parameters to predict rheology and fluid behavior in many simple flows, such as small-amplitude oscillatory flows, start-up shear, strain-rate flows, and all types of extensional flows (uniaxial, biaxial, planar extensions). Predicted rheological parameters include the relaxation modulus, G, the storage modulus, G', the loss modulus, G'', the steady shear viscosity, η_S, the elongational viscosity, η_E, and the steady and time-dependent normal stress differences, N_1 and N_2, as measured in shear flow (Papanastasiou et al., 1983; Kajiwara et al., 1995).

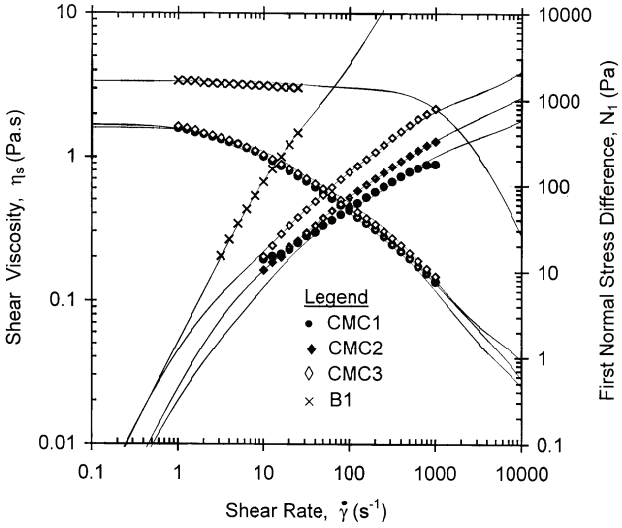

Fig. 2. *The shear viscosity η_S and normal stresses N_1 as a function of shear rate of the viscoelastic fluids considered in the simulations. The symbols correspond to the experimental viscosity data from Sullivan et al. (1987). Solid lines represent the K-BKZ model predictions with material parameters given in tables 1-4.*

Table 1. *Material parameter values used in equation 3 for fitting data of fluid CMC1 made up of 1.25% CMC in DI water (α = 2.593, β = 0.018, θ = –1/9).*

k	1	2	3	4
λ_k (s)	$5.903\cdot10^{-5}$	$1.630\cdot10^{-3}$	$3.269\cdot10^{-2}$	$3.429\cdot10^{-1}$
a_k (Pa)	$5.000\cdot10^{2}$	$1.491\cdot10^{2}$	$2.697\cdot10^{1}$	$1.516\cdot10^{0}$

Table 2. *Material parameter values used in equation 3 for fitting data of fluid CMC2 made up of 1.25% CMC and 0.005% PAA in DI water (α = 6.2562, β = 0.018, θ = –1/9).*

k	1	2	3	4
λ_k (s)	$1.486\cdot10^{-4}$	$2.067\cdot10^{-3}$	$2.107\cdot10^{-2}$	$2.603\cdot10^{-1}$
a_k (Pa)	$3.000\cdot10^{2}$	$9.096\cdot10^{1}$	$2.257\cdot10^{1}$	$3.449\cdot10^{0}$

Table 3. *Material parameter values used in equation 3 for fitting data of fluid CMC2 made up of 1.25% CMC and 0.020% PAA in DI water (α = 23.4493, β = 0.018, θ = –1/9).*

k	1	2	3	4
λ_k (s)	$1.747\cdot10^{-4}$	$6.385\cdot10^{-3}$	$7.325\cdot10^{-2}$	$1.081\cdot10^{0}$
a_k (Pa)	$2.800\cdot10^{2}$	$4.966\cdot10^{1}$	$8.013\cdot10^{0}$	$6.865\cdot10^{-1}$

Table 4. *Material parameter values used in equation 3 for fitting data of a Boger fluid B1 (α = 8000.0, β = 0.01, θ = –1/9).*

k	1	2
λ_k (s)	$2.895\cdot10^{-2}$	$2.013\cdot10^{0}$
a_k (Pa)	$1.051\cdot10^{2}$	$1.680\cdot10^{-1}$

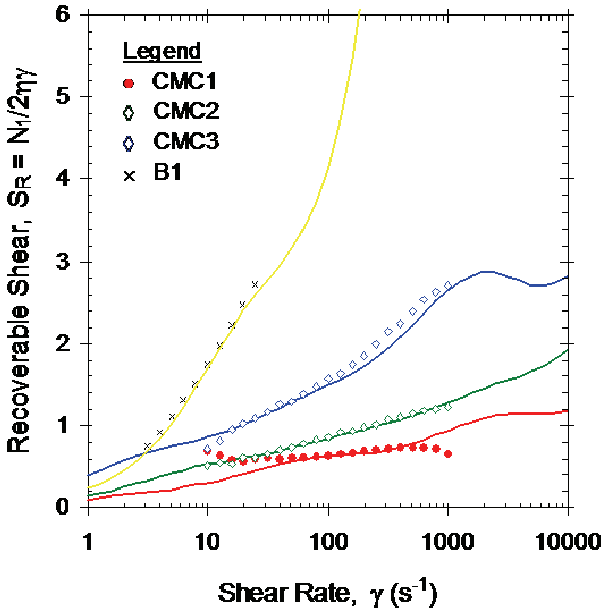

Fig. 3. *The variation of the dimensionless stress ratio (S_R) as a function of shear rate for the viscoelastic fluids considered in the simulations. The symbols correspond to the experimental data obtained by Sullivan et al. (1987). Solid lines represent the K-BKZ model predictions with material parameters given in tables 1-4.*

A measure of nonlinear viscoelasticity is the dimensionless stress ratio, S_R, defined as:

$$S_R(\dot{\gamma}) = \frac{N_1}{2\tau_w} = \frac{N_1}{2\eta\dot{\gamma}}, \qquad (5)$$

where $\dot{\gamma}$ is the shear rate and τ_w is the wall shear stress evaluated at $\dot{\gamma}$. For Newtonian fluids, S_R=0, while the value of S_R=1 for non-Newtonian viscoelastic fluids corresponds to flow conditions where elastic forces are of the same order of magnitude as viscous forces. Higher values correspond to dominance of elastic forces over viscous forces. The predictions for S_R are plotted in figure 3. As illustrated, S_R increases monotonically with $\dot{\gamma}$, particularly with the more nonlinear viscoelastic fluids. Its values reach over 2 for the highly viscoelastic CMC3 fluid at the highest shear rate value of 1000 s^{-1} during the viscometric measurement. The other two fluids (CMC1 and CMC2) have lower values, while the Boger fluid has a maximum S_R value close to 3 (the most elastic).

4. METHOD OF SOLUTION

The K-BKZ integral constitutive equation (equation 3) is solved together with the conservation equations and boundary conditions using the FEM. A special numerical scheme is used to calculate the viscoelastic stresses, which are split into a viscous component with a reference viscosity to derive a diffusive term in the momentum equation and into an elastic term, which enters the calculations as a pseudo-body force, as explained in detail by Luo and Tanner (1986). This scheme was developed further by Luo and Mitsoulis (1990a) to be valid for the general case of flows with and without recirculation. All numerical details are given in that work and are not repeated here. Galerkin discretization is maintained and the numerical algorithm for convergence is Picard iteration. Convergent solutions have been obtained independent of mesh size, provided enough elements are used and the solution procedure advances slowly from low – representing Newtonian behavior – to higher flow rates by using a flow rate increment scheme (Barakos & Mitsoulis, 1995). For flows with free surfaces, such as the blade coating flow considered here, and due to the viscoelastic nature of the polymer solutions, it was found necessary to proceed carefully and use under-relaxation for the free-surface movement. To obtain a converged solution at high roll speeds, the Adaptive Viscoelastic Stress Splitting (AVSS) scheme was implemented (Sun et al., 1996b). The computations started from the Newtonian solution at low roll speed and continued by increasing the apparent shear rate V_R/H_0 (or roll speed V_R) to reach higher values. More details for free surface flows involving Boger fluids are given in the most recent work by Mitsoulis (2010).

5. RESULTS AND DISCUSSION

The numerical simulations have been carried out for a standard geometry used by Sullivan (1986) in his experimental design apparatus (see, e.g., figure 6 of Sullivan et al., 1987). It comprises the liquid reservoir with vertical walls, the channel between the blade and the roll, and the exit region, in an effort to compare the results with the experimental findings. The domain exit has been set to around $20H_0$ to $30H_0$ from the channel exit, which was found sufficient to achieve a flat velocity profile with no further changes occurring. Details regarding grid information and code names for the designs have been given in our previous paper (Mitsoulis and Athanasopoulos, 2010) and are not repeated here.

5.1. Flow field

We shall present results for the flow field in terms of the kinematics (streamlines) and dynamics (pressures and stresses). Viscoelastic effects modify the flow field of the fluid approaching the blade nip. Figure 4 shows that viscoelastic behavior is in sharp contrast to Newtonian behavior (figure 4a), producing different flow patterns in the blade nip region. The big Newtonian vortex of figure 4a is reduced as the elasticity increases. For the geometry considered in the simulation (L1010), the deflection point of the recirculation upstream of the blade nip is being located closer to the nip entrance for the viscoelastic fluids than for the Newtonian case. The stream function has been made dimensionless and normalized as in our previous work (Mitsoulis & Athanasopoulos, 2010) by using the maximum value on the roll wall (solid circle) and the minimum value in the eye of the vortex (open circle). Viscoelasticity serves to reduce the size and intensity of recirculation.

That the deflection point of the recirculation upstream of the blade nip is being located closer to the nip entrance for the viscoelastic fluids than for the Newtonian case is further demonstrated when comparing the lines with a constant pressure (i.e., isobars) for the Newtonian fluid and the highly viscoelastic CMC3 polymer solution (figure 5). Again the maximum is shown as a solid circle and the minimum as an open circle. There is less pressure-driven flow going through the nip in the case of the CMC3 solution.

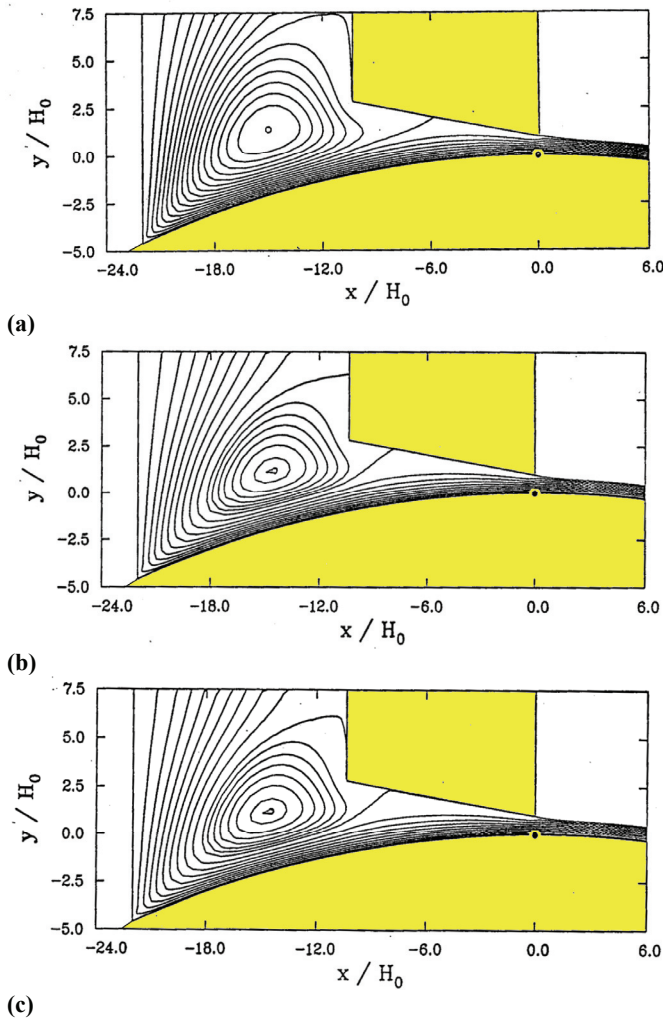

Fig. 4. *Simulation results for the flow field in design L1010 of blade coating: (a) streamlines pattern for the Newtonian fluid; (b) streamline pattern for the CMC1 viscoelastic fluid; (c) streamline pattern for the CMC2 viscoelastic fluid.*

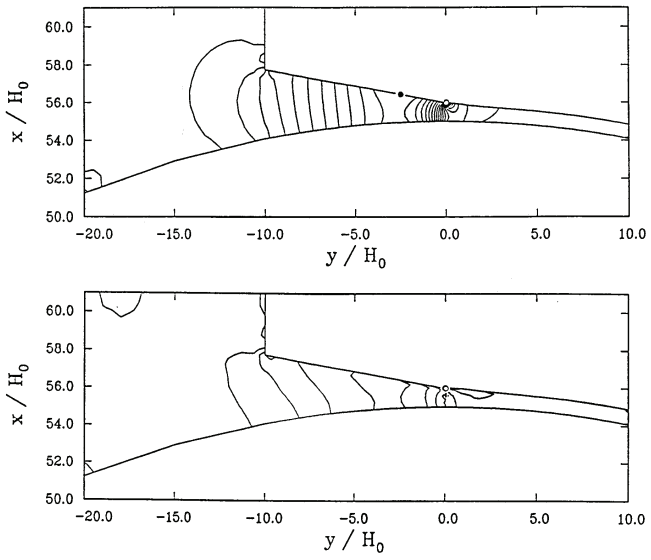

Fig. 5. *Isobars of (a) the Newtonian fluid, and (b) the highly viscoelastic polymer solution CMC3.*

The axial pressure distributions for the different fluids are shown in figure 6 in the exit from the nip region. The pressure has been made dimensionless by dividing by the reference stress $\eta_0 V_R/H_0$. For comparison purposes the results from the inelastic Carreau model (same shear viscosity) are also given. We observe that as the viscoelastic character of the fluid increases, the pressures are higher under the nip, and then at the exit (singularity) the pressures show their singular behavior with very high positive and negative values, after which on the free surface go back to zero. The latter takes a longer distance to occur the more viscoelastic the fluid is. We also observe that under the blade and due its tapered angle, a pressure increase occurs, which helps push the fluid out. This situation is reminiscent of the journal bearing flow in mechanical engineering applications.

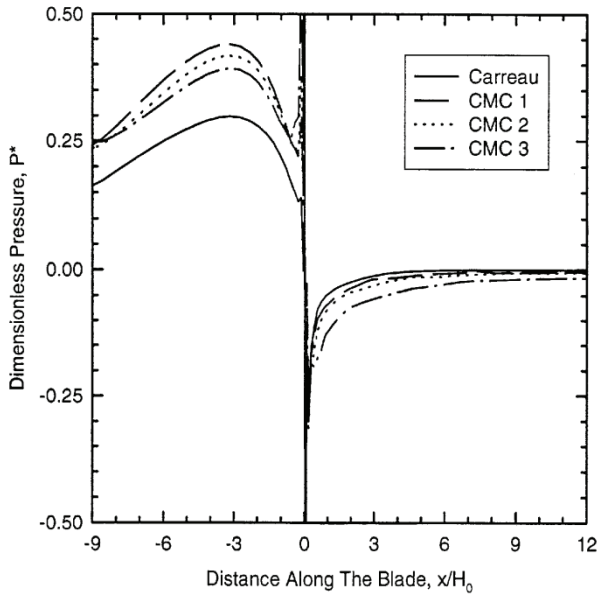

Fig. 6. *Axial pressure distributions under the blade and in the exit region for different viscoelastic polymer solutions CMC1 to CMC3 and compared with the inelastic Carreau predictions.*

5.2. Stress field

Another important aspect of viscoelasticity in blade coating is the influence of rheology on the normal (τ_{xx} and τ_{yy}) and shear (τ_{xy}) stresses inside the blade nip. The stresses have been made dimensionless by dividing by the reference stress $\eta_0 V_R/H_0$. The normal stresses give rise to the first normal-stress difference $N_1=\tau_{xx}-\tau_{yy}$, which for viscoelastic fluids can be very high (see figure 2). Normal forces increase the blade lift, or the compressive forces acting on to the substrate at the blade nip region. When the elastic character of the material increases, the normal stresses also become larger (figure 7). The increase of the stresses for the highly elastic CMC3 solution, compared to the less viscoelastic CMC1 solution, is approximately proportional to the

increase of the dimensionless stress ratio (S_R) at 1000 s^{-1}. This suggests that material elasticity contributes substantial normal forces during blade coatings, the magnitude of the forces being proportional to the elasticity at relatively high rates of shear.

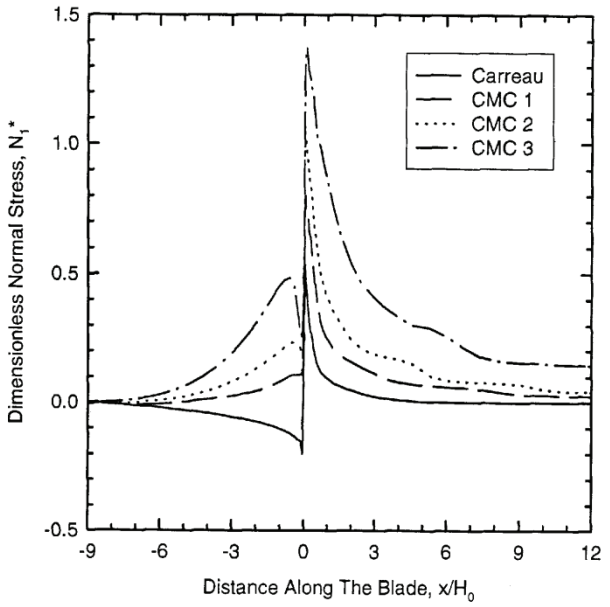

Fig. 7. *Axial first normal-stress difference N_1 distributions under the blade and in the exit region for different viscoelastic polymer solutions CMC1 to CMC3 and compared with the inelastic Carreau predictions.*

Detailed distributions of the normal stresses τ_{xx} and τ_{yy} are given in figures 8a and 8b, respectively. We observe that the dominant normal stress is the τ_{xx}, and is primarily responsible for the behavior of N_1, while τ_{yy} is an order of magnitude smaller due to the small value of θ, the second normal stress difference ratio (equation 4). The viscoelastic nature of the CMC solutions makes the stresses higher. They also need a longer distance to relax down to 0 after the exit from the blade nip than their inelastic Carreau counterparts.

The corresponding results for the shear stresses τ_{xy} are given in figure 9. Again, viscoelasticity serves to increase these values, especially towards the blade exit, due to the tapered geometry. Also after the exit the shear stresses take a longer time to relax.

5.3. Coating thickness

For a given coater geometry and operating conditions, the coating thickness depends strongly on the rheological behavior of the coating material. Compared to the Newtonian case, the coating film thickness reduces when viscoelastic effects are being introduced. The measured, from Sullivan et al. (1987), and the predicted film thicknesses appear in table 5. The predictive capability of the K-BKZ rheological model is excellent for the CMC1 and CMC2 fluids. For the CMC3 solution, simulation results overestimate the thickness by less than 10 percent, while for the Boger fluid, the simulated film thickness is 10% greater than its experimental value. The coating thickness decreases as the viscoelastic character of the coating liquid becomes stronger. The thickness also depends on roll speed, in agreement with the experimental results of Sullivan et al. (1987).

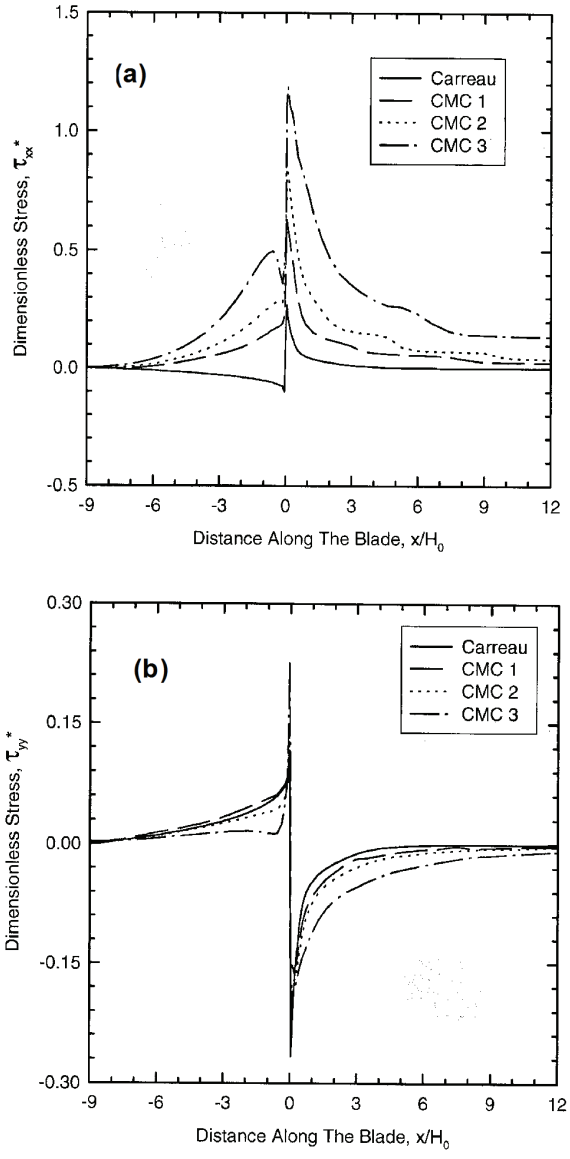

Fig. 8. *Axial normal stress (a) τ_{xx} and (b) τ_{yy} distributions under the blade and in the exit region for different viscoelastic polymer solutions CMC1 to CMC3 and compared with the inelastic Carreau predictions.*

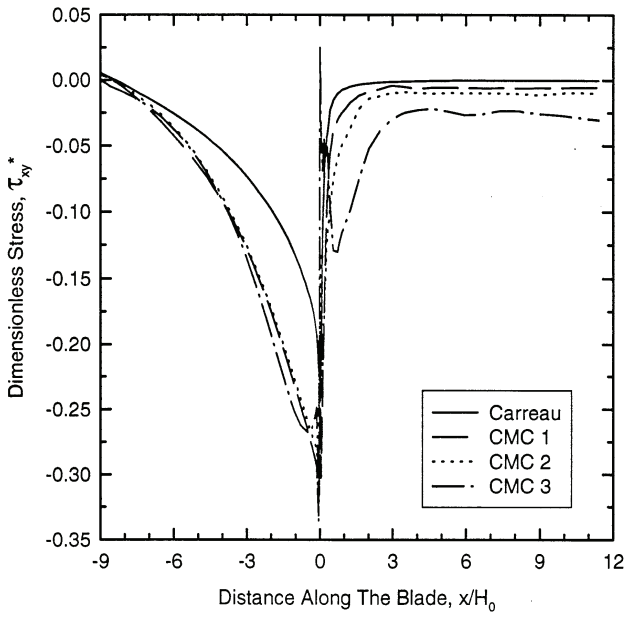

Fig. 9. *Axial shear stress τ_{xy} distributions under the blade and in the exit region for different viscoelastic polymer solutions CMC1 to CMC3 and compared with the inelastic Carreau predictions.*

Table 5. *Comparison between experimental coating thickness and model predictions for different coating materials.*

Material	h/H_0 (Experimental)*	h/H_0 (Simulation)
Newtonian, flat blade	0.60	0.60
Newtonian, 10^0-blade	0.76	0.76
CMC1, 10^0-blade	0.79	0.79
CMC2, 10^0-blade	0.71	0.70
CMC3, 10^0-blade	0.62	0.67
Boger Fluid, 10^0-blade	0.56	0.62

* Sullivan et al. (1987)

The blade nip geometry has a significant influence on the film thickness of the Newtonian fluid. When the blade tip is parallel to the tangent at the roll surface, the film is thinner than when there is a 10^o angle. A convergent channel underneath the blade tip increases the pressure-driven flow through the nip and, consequently, increases the hydrodynamic lift and film thickness. The influence of geometry was not studied for non-Newtonian fluids; hence the angle remained constant at 10^o.

When the elastic character of the CMC/PAA fluids increases (i.e., CMC solutions from 1 to 3), the film thickness decreases monotonically. For CMC1, the film thickness is slightly (by 10.5%) greater than that of the Newtonian fluid. This is consistent to the observation by Sullivan et al. (1987) who found that shear-thinning increases the film thickness. For the CMC1 fluid elasticity was relatively small, so that viscous effects dominate the film thickness. However, as the elasticity of the fluid increased from CMC1 to CMC3, the film thickness decreased. This elastic effect is reinforced by comparing the Boger and Newtonian fluids under the same blade geometry. The Boger fluid provides significantly lower film thickness, by about 26%, when compared to the purely Newtonian fluid. Since the blade is fixed and the fluid viscosity remains constant with the shear rate, the reduced film thickness is solely attributed to the elastic character of the fluid.

The results of this work demonstrate that rheological models with multiple relaxation times need to be considered in order to simulate the complex flow of non-Newtonian fluids in blade coating. The K-BKZ model represents accurately the viscoelastic rheology of the polymeric solutions of CMC with PAA. Consideration of the wide spectrum of relaxation parameters and the fading memory are therefore essential in the constitutive equation which describes the blade coating flow of these and other coating materials of practical interest.

6. SUMMARY

The blade coating process of a fixed blade over a rotating roll has been simulated numerically for viscoelastic fluids. The viscoelastic constitutive equation used was based on the K-BKZ model, which incorporates a spectrum of relaxation parameters and fading memory effects. Numerical results compare well with previous experimental data from Sullivan et al. (1987), and Sullivan and Middleman (1986). The coating film thicknesses of viscoelastic CMC/PAA fluids observed in experiments was accurately predicted by the FEM model using the K-BKZ constitutive equation. The coating film thickness for viscoelastic materials decreases as the viscoelastic character increases. This is specifically illustrated by comparing the film thicknesses of the Newtonian and the Newtonian-elastic (Boger) fluids. The latter has substantially lower film thickness than the Newtonian fluid.

The present simulations demonstrate that it is now possible to study coating flows of viscoelastic materials of practical interest. In order to apply the modeling in coating flows the key issues are: (a) proper characterization of the rheological properties of the material, and (b) incorporation of a sophisticated K-BKZ constitutive equation to describe coating rheology. Multiple relaxation parameters and

fading memory are inherent characteristics to multi-component colloidal dispersions in non-Newtonian media, such as paper coatings. It would be of interest in the future to use the K-BKZ model for simulating the flow of pigmented paper coatings in blade coating. Further modeling work is also needed to include and study the influence of slip, especially for fast moving rolls and highly concentrated dispersions.

ACKNOWLEDGEMENTS

Financial assistance from the National Technical University of Athens (NTUA) for basic research, under the code name "PEBE 2010-2012", is gratefully acknowledged.

REFERENCES

Ansari, M., Alabbas, A., Hatzikiriakos, S.G., Mitsoulis, E., 2010, Entry flow of polyethylene melts in tapered dies, *Intern. Polym. Proc.,* 25, 287-296.

Barakos, G., Mitsoulis, E., 1995, Numerical simulation of extrusion through orifice dies and prediction of Bagley correction for an IUPAC-LDPE melt, *J. Rheol.*, 39, 193-209.

Bernstein, B., Kearsley, E.A., Zapas, L., 1963, A study of stress relaxations with finite strain, *Trans. Soc. Rheol.*, 7, 391-410.

Boger, D.V., 1977/1978, A highly elastic constant-viscosity fluid, *J. Non-Newtonian Fluid Mech.*, 3, 87-91.

Dupont, S., Crochet, M.J., 1988, The vortex growth of a KBKZ fluid in an abrupt contraction, *J. Non-Newtonian Fluid Mech.*, 29, 81-91.

Greener, Y., Middleman, S., 1974, Blade coating of a viscoelastic fluid, *Polym. Eng. Sci.*, 14, 791-797.

Hsu, T.C., Malone, M., Laurence, R.L., 1985, A solver for time-dependent viscoelastic fluid-flows, *J. Non-Newtonian Fluid Mech.*, 18, 273-294.

Hsu, T.C., 1986, *A study of the role of fluid viscoelasticity in the dynamics of bounded coating flows*, PhD Dissertation, University of Massachusetts, MA, USA.

Kajiwara, T., Barakos, G., Mitsoulis, E., 1995, Rheological characterization of polymer solutions and melts with an integral constitutive equation, *Int. J. Polymer Analysis & Characterization*, 1, 201-215.

Keunings, R., 2003, Finite element methods for integral viscoelastic fluids, *Rheology Reviews*, eds, Binding, D.M., Walters, K., British Society of Rheology, London, UK, 167-195.

Kistler, S.F., Scriven, L.E., 1984, Coating flow theory by finite element and asymptotic analysis of the Navier-Stokes system, *Int. J. Num. Meth. Fluids*, 4, 207-229.

Loest, H., Lipp, R., Mitsoulis, E., 1994, Numerical flow simulation of viscoplastic slurries and design criteria for a tape casting unit, *J. Amer. Ceram. Soc.*, 77, 254-262.

Luo, X.-L., Mitsoulis, E., 1990a, An efficient algorithm for strain history tracking in finite element computations of non-Newtonian fluids with integral constitutive equations, *Int. J. Num. Meth. Fluids*, 11, 1015-1031.

Luo, X.-L., Mitsoulis, E., 1990b, A numerical study of the effect of elongational viscosity on vortex growth in contraction flows of polyethylene melts, *J. Rheol.*, 34, 309-342.

Luo, X.-L., Tanner, R.I., 1986, A streamline element scheme for solving viscoelastic flow problems, Part II. Integral constitutive models, *J. Non-Newtonian Fluid Mech.*, 22, 61-89.

Luo, X.-L., Tanner, R.I., 1988, Finite element simulation of long and short circular die extrusion experiments using integral models, *Int. J. Num. Meth. Eng.*, 25, 9-22.

Mitsoulis, E., 1990, Numerical simulation of viscoelastic fluids, *Encyclopedia of Fluid Mechanics*, 9, *Polymer Flow Engineering*, eds, Cheremisinoff, N.P., Gulf Publ. Co., Dallas, Texas, USA, 649-704.

Mitsoulis, E., 2010, Extrudate swell of Boger fluids, *J. Non-Newtonian Fluid Mech.*, 165, 812-824.

Mitsoulis, E., Athanasopoulos, G., 2010, Numerical simulation of blade-over-roll coating forming flows, *Comp. Meth. Mater. Sci.,* 10 (4), 214-224.

Mitsoulis, E., Hatzikiriakos, S.G., 2003, Bagley correction: The effect of contraction angle and its prediction, *Rheol. Acta*, 42, 309-320.

Mitsoulis, E., Wagner, R., Heng, F.L., 1988, Numerical simulation of wire-coating low-density polyethylene: theory and experiments, *Polym. Eng. Sci.*, 28, 291-310.

Olsson, F., 1994, A solver for time-dependent viscoelastic fluid-flows, *J. Non-Newtonian Fluid Mech.*, 51, 309-340.

Olsson, F., Isaksson, P., 1995, The influence of viscoelastic rheology on blade coating as revealed by numerical methods, *Nordic Pulp Paper Res. J.*, 10, 234-244.

Papanastasiou, A.C., Scriven, L.E., Macosko, C.W., 1983, An integral constitutive equation for mixed flows: viscoelastic characterization, *J. Rheol.*, 27, 387-410.

Park, H.J., Mitsoulis, E., 1992, Numerical Simulation of Circular Entry Flows of Fluid M1 Using an Integral Constitutive Equation, *J. Non-Newtonian Fluid Mech*., 42, 301-314.

Strenger, M.R., Secor, R.B., Sramek, R.J., 1992, Knife coating of viscoelastic material, *6th International Coating Process Science and Technology Symposium*, AIChE National Meeting, 112-113.

Sullivan, T., 1986, *An experimental and computational investigation of rheological effects in blade coating*, PhD Thesis, University of California, San Diego, CA, USA.

Sullivan, T., Middleman, S., 1986, Film thickness in blade coating of viscous and viscoelastic liquids, *J. Non-Newtonian Fluid Mech.*, 21, 13-38.

Sullivan, T., Middleman, S., Keunings, R., 1987, Use of a finite-element method to interpret rheological effects in blade coating, *AIChE J.*, 33, 2047-2056.

Sun, J., Phan-Thien, N., Tanner, R.I., 1996a, An adaptive viscoelastic stress splitting scheme and its applications: AVSS/SI and AVSS/SUPG, *J. Non-Newtonian Fluid Mech.*, 65, 75-91.

Sun, J., Phan-Thien, N., Tanner, R.I., 1996b, Extrudate swell through an orifice die, *Rheol. Acta*, 35, 1-12.

NUMERYCZNA SYMULACJA FORMOWANIA POKRYCIA PRZEZ OSTRZE PRZEMIESZCZAJĄCE SIĘ NAD WALCEM

Streszczenie

W pracy przeprowadzono numeryczne symulacje metodą elementów skończonych (MES) dla płynięcia w czasie formowania pokrycia, stosując ostrze przemieszczające się nad walcem. 2-wymiarowa domena rozwiązania obejmuje zarówno pojemnik z cieczą formującą pokrycie jak i obszar wokół ostrza z powierzchnią swobodną. Materiałem jest traktowany jako ciecz Niutonowska polimer, charakteryzujący się mięknięciem przy ścinaniu, który wcześniej był wykorzystany w badaniach doświadczalnych i teoretycznych. Pseudoplastyczność cieczy polimerowych jest opisana przez model Carreau, który dobrze oddaje dane doświadczalne dla lepkości zależnych od ścinania. Płynięcie polimeru jest analizowane dla różnych prędkości walca i określany jest rozmiar i kształt strefy recyrkulacji. W zbiorniku pojawiają się duże wiry, a ich intensywność jest obliczana dla różnych warunków procesu i kształtów ostrza. Obliczone kształtny swobodnych powierzchni oraz grubości są zgodne z danymi doświadczalnymi. W wyniku ścinania zmniejsza się lepkość i wzrasta grubość pokrycia dla danej geometrii narzędzi, co zaobserwowano również w doświadczeniu. Ten wzrost występuje dla wykładnika w prawie potęgowym $n > 0.3$, podczas gdy intensywne mięknięcie przez ścinanie ($n < 0.3$) zmniejsza tą grubość. Te obserwacje również zgadzają się z wynikami wcześniejszych badań dla innych kształtów i dla płynów charakteryzujących się znacznym mięknięciem przez ścinanie. Wraz ze wzrostem n w zakresie $1 \geq n > 0$ zmniejsza się wir zarówno pod względem wymiaru jak i intensywności. Symulacje dostarczyły także szeregu informacji odnośnie naprężeń i ciśnień. Zaobserwowano, że niektóre kształty narzędzi w operacji powlekania pokryciami są lepsze od innych. Ze względu na połączenie mechaniki płynów z mięknięciem w wyniku ścinania, która pojawia się w polu przepływu, geometria przepływu jest interesującym przykładem dla symulacji i projektowania. Kształt przepływu jest interesującym przykładem dla symulacji i projektowania.

Received: June 15, 2010
Received in a revised form: November 9, 2010
Accepted: November 10, 2010